GOCE DELCEV UNIVERSITY - STIP
FACULTY OF COMPUTER SCIENCE

The journal is indexed in
EBSCO

ISSN 2545-4803 on line
DOI: 10.46763/BJAMI

BALKAN JOURNAL OF APPLIED MATHEMATICS AND INFORMATICS (BJAMI)

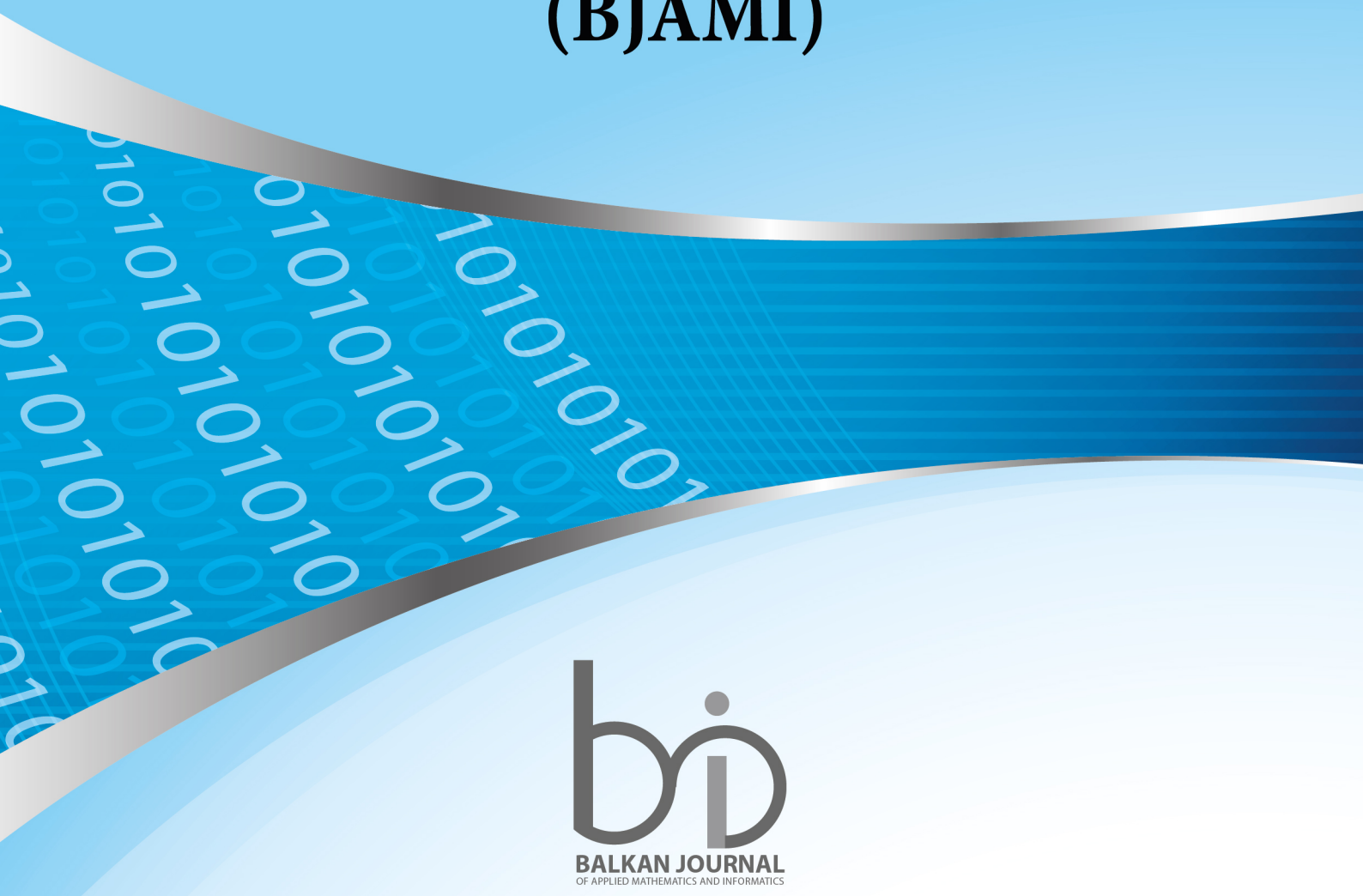

BALKAN JOURNAL
OF APPLIED MATHEMATICS AND INFORMATICS

YEAR 2022

VOLUME V, Number 1

GOCE DELCEV UNIVERSITY - STIP
FACULTY OF COMPUTER SCIENCE

ISSN 2545-4803 on line

BALKAN JOURNAL OF APPLIED MATHEMATICS AND INFORMATICS

(BJAMI)

YEAR 2022 VOLUME V, Number 1

AIMS AND SCOPE:
BJAMI publishes original research articles in the areas of applied mathematics and informatics.

Topics:
1. Computer science;
2. Computer and software engineering;
3. Information technology;
4. Computer security;
5. Electrical engineering;
6. Telecommunication;
7. Mathematics and its applications;
8. Articles of interdisciplinary of computer and information sciences with education, economics, environmental, health, and engineering.

Managing editor
Biljana Zlatanovska Ph.D.

Editor in chief
Zoran Zdravev Ph.D.

Lectoure
Snezana Kirova

Technical editor
Sanja Gacov

Address of the editorial office
Goce Delcev University – Stip
Faculty of philology
Krste Misirkov 10-A
PO box 201, 2000 Štip,
Republic of North Macedonia

BALKAN JOURNAL
OF APPLIED MATHEMATICS AND INFORMATICS (BJAMI), Vol 3

ISSN 2545-4803 on line
Vol. 5, No. 1, Year 2022

EDITORIAL BOARD

Adelina Plamenova Aleksieva-Petrova, Technical University – Sofia,
Faculty of Computer Systems and Control, Sofia, Bulgaria
Lyudmila Stoyanova, Technical University - Sofia , Faculty of computer systems and control,
Department – Programming and computer technologies, Bulgaria
Zlatko Georgiev Varbanov, Department of Mathematics and Informatics,
Veliko Tarnovo University, Bulgaria
Snezana Scepanovic, Faculty for Information Technology,
University "Mediterranean", Podgorica, Montenegro
Daniela Veleva Minkovska, Faculty of Computer Systems and Technologies,
Technical University, Sofia, Bulgaria
Stefka Hristova Bouyuklieva, Department of Algebra and Geometry,
Faculty of Mathematics and Informatics, Veliko Tarnovo University, Bulgaria
Vesselin Velichkov, University of Luxembourg, Faculty of Sciences,
Technology and Communication (FSTC), Luxembourg
Isabel Maria Baltazar Simões de Carvalho, Instituto Superior Técnico,
Technical University of Lisbon, Portugal
Predrag S. Stanimirović, University of Niš, Faculty of Sciences and Mathematics,
Department of Mathematics and Informatics, Niš, Serbia
Shcherbacov Victor, Institute of Mathematics and Computer Science,
Academy of Sciences of Moldova, Moldova
Pedro Ricardo Morais Inácio, Department of Computer Science,
Universidade da Beira Interior, Portugal
Georgi Tuparov, Technical University of Sofia Bulgaria
Dijana Karuovic, Tehnical Faculty "Mihajlo Pupin", Zrenjanin, Serbia
Ivanka Georgieva, South-West University, Blagoevgrad, Bulgaria
Georgi Stojanov, Computer Science, Mathematics, and Environmental Science Department
The American University of Paris, France
Iliya Guerguiev Bouyukliev, Institute of Mathematics and Informatics,
Bulgarian Academy of Sciences, Bulgaria
Riste Škrekovski, FAMNIT, University of Primorska, Koper, Slovenia
Stela Zhelezova, Institute of Mathematics and Informatics, Bulgarian Academy of Sciences, Bulgaria
Katerina Taskova, Computational Biology and Data Mining Group,
Faculty of Biology, Johannes Gutenberg-Universität Mainz (JGU), Mainz, Germany.
Dragana Glušac, Tehnical Faculty "Mihajlo Pupin", Zrenjanin, Serbia
Cveta Martinovska-Bande, Faculty of Computer Science, UGD, Republic of North Macedonia
Blagoj Delipetrov, European Commission Joint Research Centre, Italy
Zoran Zdravev, Faculty of Computer Science, UGD, Republic of North Macedonia
Aleksandra Mileva, Faculty of Computer Science, UGD, Republic of North Macedonia
Igor Stojanovik, Faculty of Computer Science, UGD, Republic of North Macedonia
Saso Koceski, Faculty of Computer Science, UGD, Republic of North Macedonia
Natasa Koceska, Faculty of Computer Science, UGD, Republic of North Macedonia
Aleksandar Krstev, Faculty of Computer Science, UGD, Republic of North Macedonia
Biljana Zlatanovska, Faculty of Computer Science, UGD, Republic of North Macedonia
Natasa Stojkovik, Faculty of Computer Science, UGD, Republic of North Macedonia
Done Stojanov, Faculty of Computer Science, UGD, Republic of North Macedonia
Limonka Koceva Lazarova, Faculty of Computer Science, UGD, Republic of North Macedonia
Tatjana Atanasova Pacemska, Faculty of Computer Science, UGD, Republic of North Macedonia

CONTENT

Aleksandra Risteska-Kamcheski and Vlado Gicev
DEPENDENCE OF INPUT ENERGY FROM THE LEVEL OF
GROUND NONLINEARITY 7

Aleksandra Risteska-Kamcheski and Vlado Gicev and Mirjana Kocaleva
DEPENDENCE OF INPUT ENERGY FROM THE RIGIDITY OF THE FOUNDATION 19

Sara Aneva and Vasilija Sarac
MODELING AND SIMULATION OF SWITCHED RELUCTANCE MOTOR 31

Blagica Doneva, Marjan Delipetrev, Gjorgi Dimov
PRACTICAL APPLICATION OF THE REFRACTION METHOD 43

Marija Sterjova and Vasilija Sarac
REVIEW OF THE SCALAR CONTROL STRATEGY OF AN INDUCTION
MOTOR: CONSTANT V/f METHOD FOR SPEED CONTROL 57

Katerina Anevska, Valentina Gogovska, Risto Malcheski
WORKING WITH MATHEMATICALLY GIFTED STUDENTS AGED 16-17.....69

Goce Stefanov, Maja Kukuseva Paneva, Sara Stefanova
INTEGRATED RF-WIFI SMART SENSOR NETWORK 81

Sadani Idir
SOLUTION AND STABILITY OF A NEW RECIPROCAL
TYPE FUNCTIONAL EQUATION 93

Balkan Journal of Applied Mathematics and Informatics
Volume V Number 1 Year 2022
Online ISSN 2545-4803
UDC: 621.313.13:004.942

MODELING AND SIMULATION OF SWITCHED RELUCTANCE MOTOR

SARA ANEVA AND VASILIJA SARAC

Abstract. The main focus of the paper is modeling of the Switched Reluctance Motor (SRM) in Simulink modules of Matlab software, under various operating conditions (no load and the rated load). Special emphasis is placed on the working principles of SRM and its characteristics which are the starting point for obtaining motor transient characteristics at various operating regimes. A simulation of SRM model in Simulink is presented and its operation is explained. The basic SRM model in Simulink operates with converter turn-on and turn-off angles of 45° and 75°. Next, on this model, the converter turn-on and turn-off angles were modified. Based on these new simulations, the values of the flux, current and torque are presented as well as the transient characteristics of speed for various angles of operation of the power converter and appropriate conclusions are drawn. A load of 50 Nm has been added to the basic model of SRM and the obtained operating characteristics of the motor are presented. Finally, the impact of the load on the characteristics of the motor is explained.

1. Introduction

The switched reluctance drive was developed in the 1980s to offer advantages in terms of efficiency, power per unit weight and volume, robustness, and operational flexibility. The motor and its associated power electronic converter must be designed as an integrated unit, and optimized for a particular specification, e.g., for maximum overall efficiency with a specific load, or maximum speed range, peak short-term torque, or torque ripple. Despite being relatively new, this technology has been used in a range of applications which can benefit from its performance characteristics including general purpose industrial drives, compressors, and domestic appliances. If an iron rotor with poles, but without any conductors, is fitted into a multi-phase stator, a switched reluctance motor, capable of synchronizing with the stator field is obtained. When a pair of stator coils is energized, the rotor will start to rotate until it reaches the position where there is the lowest magnetic reluctance. A switched reluctance motor (SRM) is also known as a variable reluctance motor. The reluctance of the rotor with respect to the stator flux path varies with the position of the rotor, i.e., reluctance is a function of a rotor position in a variable reluctance motor. In this paper, a 60 kW, SRM in 6/4 configuration is analyzed in Simulink. Transient operating characteristics of current, flux, speed and torque are obtained for different control angles of the power converter. Motor operation is analyzed up to the base speed and above it. Also, motor operation with the load is presented. Adequate conclusion related to the values of current, speed and torques in correlation to the control angles of power converter are derived. The impact of load to the motor operating characteristics is analyzed as well

Date: April, 2022.
Keywords. Switched Reluctance Motor, turn-on and turn-off angles, Flux Characteristic, Current Characteristic, Torque Characteristic, Speed Characteristic.

2. Theoretical background

2.1 Operation principle and characteristics

The SRM has projecting poles on both rotor and stator. However, most SRM are of much higher power than the largest stepper motor, therefore in the higher power ranges (where the winding resistances become much less significant), the doubly-salient arrangement is very effective as far as efficient electromagnetic energy conversion is concerned. A typical SRM is shown in Fig. 1: the analyzed motor has twelve stator poles and eight rotor poles, and represents a widely used arrangement, but other pole combinations can be also used in different applications. The stator windings are wound around each pole, while the rotor, which is made of laminations, has no windings or magnets and is therefore cheap to manufacture and extremely robust [2].

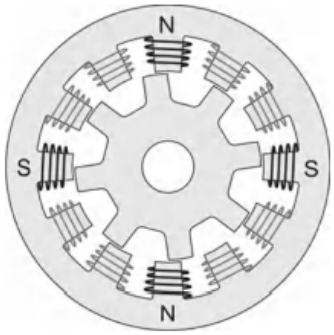

Figure 1. *Typical Switched Reluctance Motor [1]-[2]*

In Fig. 1 each of the twelve stator poles carries a concentrated winding, while the eight-pole rotor has no windings or magnets. The twelve coils are grouped to form three phases, which are independently energized from a 3-phase converter. The motor rotates by exciting the phases sequentially in the sequence A, B, C for anticlockwise rotation or A, C, B for clockwise rotation, the 'nearest' pair of rotor poles being pulled into alignment with the appropriate stator poles by reluctance torque action. In Figure 1 the four coils forming phase A are shown in black, the polarities of the coil m.m.f.s being indicated by the letters N and S on the back of the core. Each time a new phase is excited, the equilibrium position of the rotor advances by 15°, so after one complete cycle (i.e., after each of the three phases has been excited once) the angle turned through is 45°. The machine therefore rotates once for eight fundamental cycles of the power supply to the stator windings, so in terms of the relationship between the fundamental supply frequency and the speed of rotation, the machine in Fig. 1 behaves as a 16-pole conventional machine [1]. Since the torque characteristics are dependent on the relationship between flux linkages and rotor position as a function of current, it is worthwhile to conceptualize the control possibilities and limitations of this motor drive. For example, a typical phase inductance vs. rotor position for a fixed phase current is shown in Fig. 2. The inductance corresponds to that of a stator-phase coil of the switched reluctance motor neglecting the fringe effect and saturation. The significant inductance profile changes are determined in terms of the stator and rotor pole arcs and number of rotor poles. The rotor pole arc is

assumed to be greater than the stator pole arc for this illustration, which is usually the case [3].

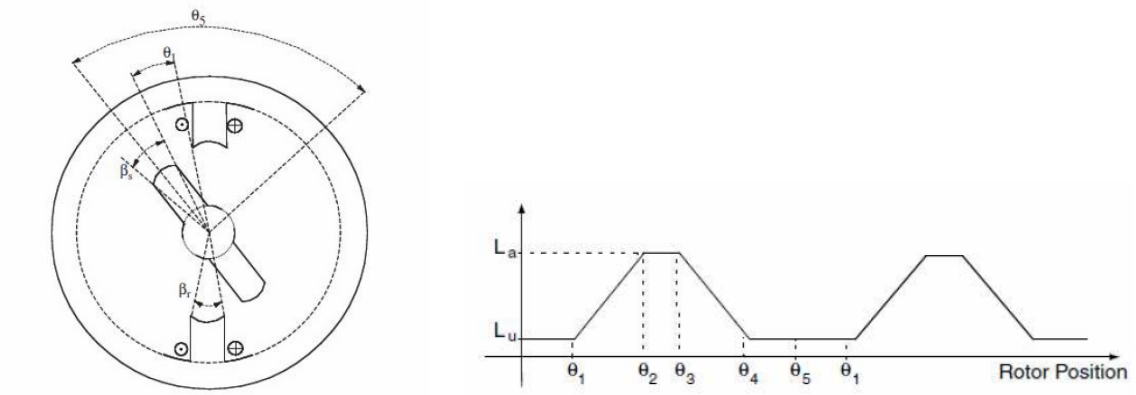

(a) (b)

Figure 2. *Derivation of inductance vs. rotor position from rotor and stator pole arcs for an unsaturated switched reluctance machine. (a) Basic rotor position definition in a two pole SRM. (b) Inductance profile [3]*

From Figs. 2 a and b, the various angles are derived as:

$$\theta_1 = 1/2\left[2\pi/P_r - \left(\beta_s + \beta_r\right)\right] \quad (1)$$

$$\theta_2 = \theta_1 + \beta_s \quad (2)$$

$$\theta_3 = \theta_2 + \left(\beta_r - \beta_s\right) \quad (3)$$

$$\theta_4 = \theta_3 + \beta_s \quad (4)$$

$$\theta_5 = \theta_4 + \theta_1 = 2\pi/P_r \quad (5)$$

Where β_s and β_r are stator and rotor pole arcs, respectively, and P_r is the number of rotor poles.

Four distinct inductance regions emerge:

1. **$0 - \theta_1$ and $\theta_4 - \theta_5$:** The stator and rotor poles are not overlapping in this region and the flux is predominantly determined by the air path, thus making the inductance minimum and almost a constant. Hence, these regions do not contribute to torque production. The inductance in this region is known as unaligned inductance, L_u [3].
2. **$\theta_1 - \theta_2$:** Poles overlap, so the flux path is mainly through stator and rotor laminations. This increases the inductance with the rotor position, giving it a positive slope. A current impressed in the winding during this region produces a positive (i.e., motoring) torque. This region comes to an end when the overlap of poles is complete [3].
3. **$\theta_2 - \theta_3$:** During this period, the movement of rotor pole does not alter the complete overlap of the stator pole and does not change the dominant flux path. This has

the effect of keeping the inductance maximum and constant, and this inductance is known as aligned inductance, L_a. As there is no change in the inductance in this region, torque generation is zero even when a current is present in this interval. Despite this fact, it serves as a useful function by providing time for the stator current to come to zero or to the lower levels when it is commutated, thus preventing negative torque generation for the part of the time if the current has been decaying in the negative slope region of the inductance [3].

4. **$\theta_3 - \theta_4$:** The rotor pole is moving away from overlapping the stator pole in this region. This is very much like the $\theta_1 - \theta_2$ region, but it has decreasing inductance and increasing rotor position contributing to a negative slope of the inductance region. The operation of the machine in this region results in negative torque (i.e., generation of electrical energy from mechanical input to the switched reluctance machine) [3].

It is not possible to achieve the ideal inductance profiles shown in Fig. 2 in an actual motor due to saturation. Saturation causes the inductance profile to curve near the top and thus reduces the torque constant [3]. Torque–speed plane of an SRM drive can be divided into three regions as shown in Fig. 3. The constant torque region is the region below the base speed ω_b, which is defined as the highest speed when maximum rated current can be applied to the motor at rated voltage with fixed firing angles. In other words, ω_b is the lowest possible speed for the motor to operate at its rated power [3].

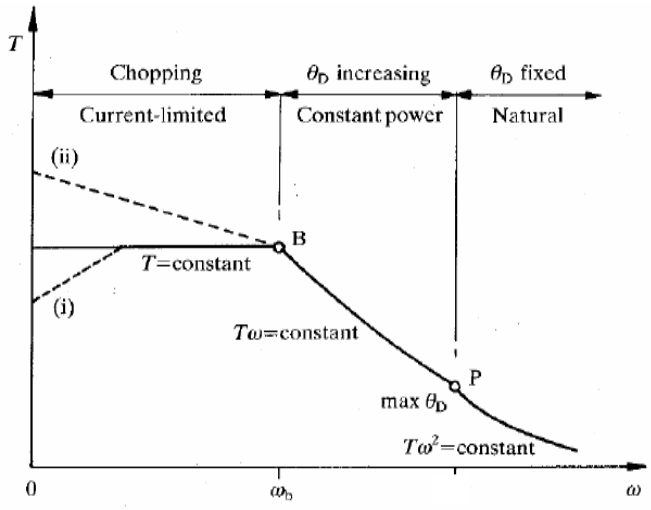

Figure 3. *Torque Speed characteristic of SRM [3]*

Region 1

In the low-speed region of operation, the current rises almost instantaneously after turn-on, since the back-emf is small. The current can be set at any desired level by means of regulators, such as hysteresis controller or voltage PWM (pulse width modulation) controller. As the motor speed increases, the back-emf soon becomes comparable to the DC bus voltage and it is necessary to phase advance-the turn-on angle so that the current

can rise to the desired level against a lower back-emf. Maximum current can still be forced into the motor by PWM or chopping control to maintain the maximum torque production [3].

Region 2

When the back-emf exceeds the DC bus voltage in high-speed operation, the current starts to decrease, once pole overlap begins and PWM or chopping control is no longer possible. The natural characteristic of the SRM, when operated with fixed supply voltage and fixed conduction angle θ_{dwell} (also known as the dwell angle), is that the phase excitation time falls off inversely with speed and so does the current. Since the torque is roughly proportional to the square of the current, the natural torque–speed characteristic can be defined by $T \propto 1/\omega^2$. Increasing the conduction angle can increase the effective amps delivered to the phase. The torque production is maintained at a level high enough in this region by adjusting the conduction angle θ_{dwell} with the single-pulse mode of operation. The controller maintains the torque inversely proportional to the speed; hence, this region is called the constant power region. The conduction angle is increased by advancing the turn-on angle until the θ dwell reaches its upper limit at speed ω_p. The medium speed range through which constant power operation can be maintained is quite wide and very high maximum speeds can be achieved [3].

Region 3

The θ_{dwell} upper limit is reached when it occupies half the rotor pole-pitch, i.e., half the electrical cycle. θ_{dwell} cannot be increased further because otherwise the flux would not return to zero and the current conduction would become continuous. The torque in this region is governed by the natural characteristics, falling off as $1/\omega^2$. The torque–speed characteristics of the SRM are like those of a DC series motor, which is not surprising considering that the back-emf is proportional to current, and the torque is proportional to the square of the current [3].

2.2 Control strategies

Despite the other electrical machines drives which use symmetrical power converters, an asymmetric power converter should be used to control the SRM. Depending on the number of machine's phases, a power processing unit can be designed to control each phase independently. Fig. 4 represents one of the most used converter topologies [4].

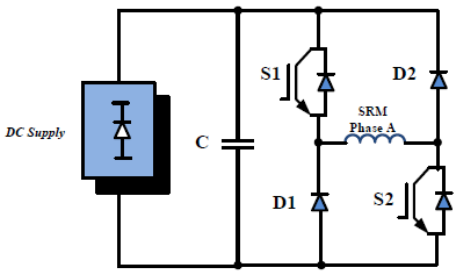

Figure 4. *Power convertor unit of SRM: asymmetric H-bridge converter [4]*

The procedure is to build up a current by turning on both transistors simultaneously, so that the poles of the rotor can be forced towards an aligned position. To maintain the

current value within a hysteresis band almost near to its reference value, when the poles are aligned, both transistors should be switched off. Then the current flows into the DC bus through the diodes and there is a large energy stored in the magnetic field of the coil and it must be sent back to the DC source, consequently the current decreases in magnitude. As mentioned earlier, in a switched reluctance motor, the rotor position plays a necessary operational role. The turning on, θ_{on}, and turning off, θ_{off}, angles must be chosen to build up a current and then let it decays to operate the motor [4].

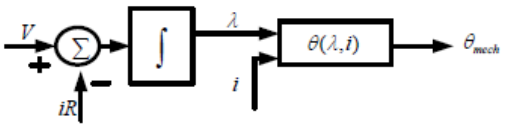

Figure 5. *Estimation of the rotor position by flux linkage [4]*

Fig. 5 shows how the rotor position can be estimated by computation of the flux linkage of an energized phase and by integrating the difference between the applied phase voltage and voltage drop on the resistance of the winding. It means that the flux linkage as a function of the phase current determines the rotor position [4].

In this paper a 60 kW, 6/4 SRM is analyzed. The Simulink model of SRM is based on the measured magnetization curves presented in Fig. 6.

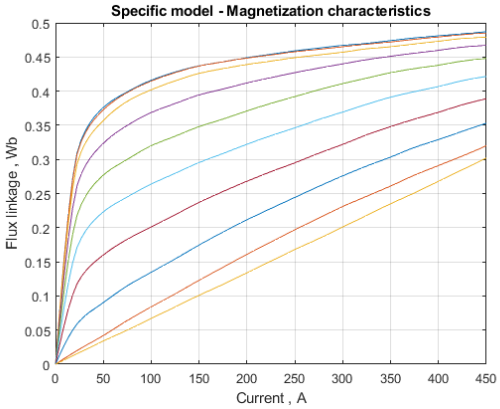

Figure 6. *Magnetization curves for analyzed motor model*

Two most common control strategies are as follows

1- Voltage source control

2- Current controller

In the first method, the *voltage source technique,* the control is implemented by applying the voltage source to a phase winding at turning on angle θ_{on} until a turning off angle θ_{off}. Then, the applied voltage is controlled directly by a speed controller which estimates the speed error after comparison of the desired speed with actual speed and then generates the required phase voltage [4].

In the second method, the *current controller technique*, the applied voltage utilized to the machine phases is modulated to achieve the desired current at the energized phase. Then, this applied voltage is monitored by a current controller with an external speed

control loop. The speed controller evaluates the speed error after comparison of the desired speed with actual speed and then generates the reference for the phase current. Then, the current controller estimates the difference between the desired and actual phase current and determines the proper duty cycle [4]. Note that in this method the actual current is permitted to change around the desired reference current according to the permissible current ripple in the tolerance band. In fact, the actual current should be forced to stay within a tolerance band. Hence, the actual current surpasses either the upper or lower boundary of the tolerance band; the controller modifies the state so that the current returns to the reference value [4].

3. **Research Methodology**

This paper analyzes the transient characteristics of SRM when the converter's turn-on and turn-off angles are changed and when a load of 50 Nm is added to the basic model of SRM in Simulink presented in Fig. 7. Fig. 7 shows the basic model of SRM drive in Simulink which means the tuning-on and off angle is 45° and 75° respectively, and no load is coupled to the motor.

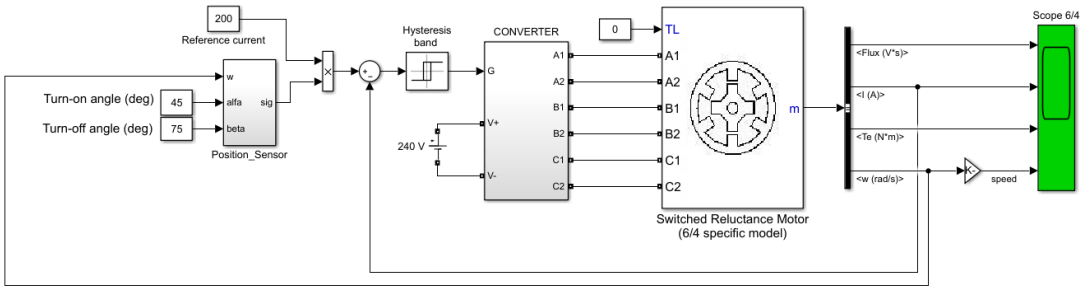

Figure 7. *Basic model of SRM in Simulink*

The SRM is fed by a three-phase power converter having three legs, each of which consists of two IGBTs and two free-wheeling diodes. During conduction periods, the active IGBTs apply positive source voltage to the stator windings to drive positive currents into the phase windings. During free-wheeling periods, negative voltage is applied to the windings and the stored energy is returned to the power DC source through the diodes. The fall time of the currents in motor windings can be thus reduced. By using a position sensor attached to the rotor, the turn-on and turn-off angles of the motor phases can be accurately imposed. These switching angles can be used to control the developed torque waveforms. The phase currents are independently controlled by three hysteresis controllers which generate the IGBTs drive signals by comparing the measured currents with the references. The IGBTs switching frequency is mainly determined by the hysteresis band [5]. The optimum pair switching angles is the one that gives the best performance of SRM drive on full load at rated speed. The phase windings are excited by a constant reference current, in our case with a value of 200 A. This allows that only the values of the switching angles decide the motor performance. The magnitude of reference current is kept at its maximum permissible value to allow the SRM to develop maximum

possible electromagnetic torque with a given pair of turn-on and turn-off angles. The pair that brings the SRM to the rated speed in the minimum time is selected and the switching angles in their neighborhoods are than further investigated [6].

4. Results and Discussion

Fig. 8 presents the characteristics of SRM for flux, current, torque and speed for the starting model at no-load operating mode and turn-on, turn-off angles: 45°, 75° respectively.

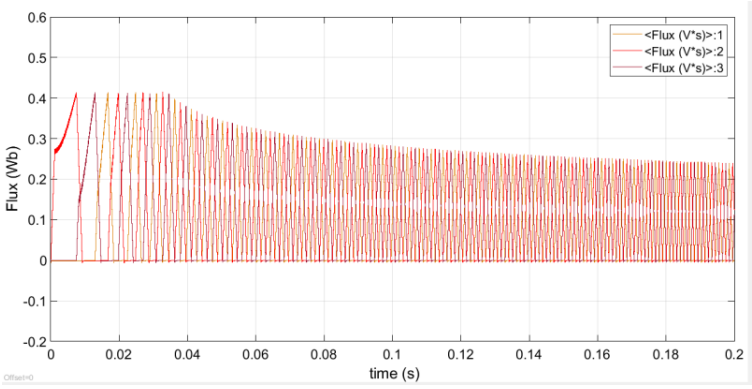

a) Flux characteristic

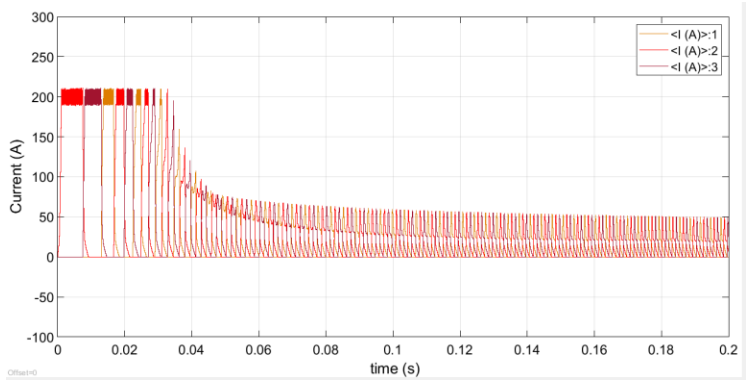

b) Current characteristic

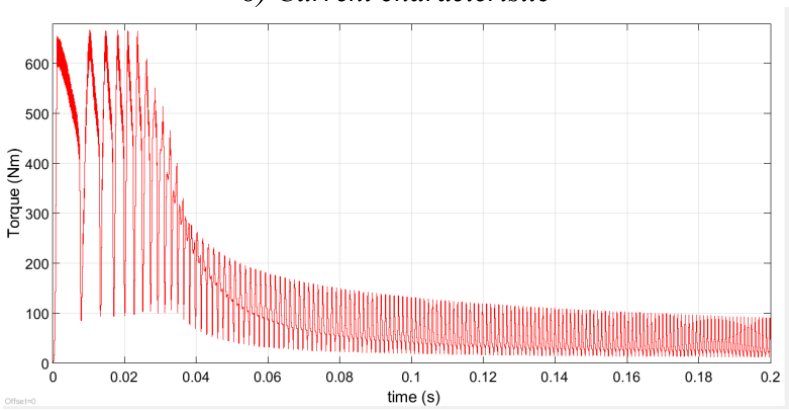

c) Torque characteristic

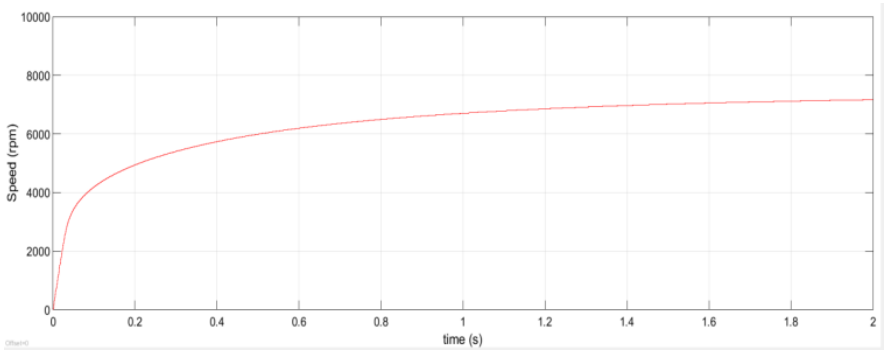

d) Speed characteristic

Figure 8. *Transient characteristics (turn-on, turn-off angles: 45°, 75°) at no load*

In this example, a DC supply voltage of 240 V is used. The converter turn-on and turn-off angles are kept constant at 45° and 75°, respectively, over the speed ranges. The amount of the reference current is 200 A and the hysteresis band is chosen as +-10 A. The SRM is started by applying the step reference to the regulator input. The acceleration rate depends on the load characteristics. In the above presented characteristics, the simulation was done at no-load. As can be noted, the SRM torque has a very high torque ripple component which is due to the transitions of the currents from one phase to the following one. This torque ripple is a particular characteristic of the SRM and it depends mainly on the converter's turn-on and turn-off angles. In SRM drives, both the average torque and torque ripple are affected by the turn-on and turn-off angles and by the current waveforms in the motor phases [5]. On the previously described SRM model the converter's turn-on and turn-off angles are changed, i.e., the simulation was done with a different pair of angles (40°,70°), and then yet with another different pair of angles (50°, 80°) and adequate conclusions are drawn. Finally, a load of 50 Nm was added to the basic model without changing the control angles (45°, 75°) and motor transient characteristics for load condition were obtained. The maximum values of the flux, current and torque when motor reaches the steady state operation, from the performed simulations in Simulink is presented in Table 1. The speed characteristics for all three no-load operating modes are presented in Fig. 9. Fig. 10 shows the transient characteristics of speed for operating modes with load and no-load for turn-on and turn-off angles of 45° and 75° respectively.

Table 1. *Flux, current and torque in steady state operation*

	Flux (Wb)	Current (A)	Torque (Nm)
turn-on; turn-off angles: 40°,70°; no load	0.2	75	150
turn-on; turn-off angles: 50°,80°; no load	0.3	25	25
turn-on; turn-off angles: 45°,75°; load = 50 Nm	0.28	60	130

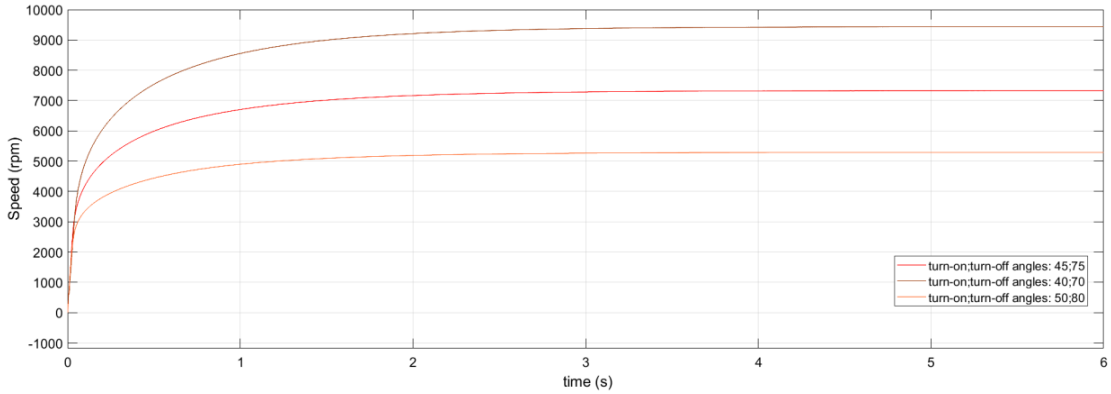

Figure 9. *Speed characteristics for all three no-load operating modes*

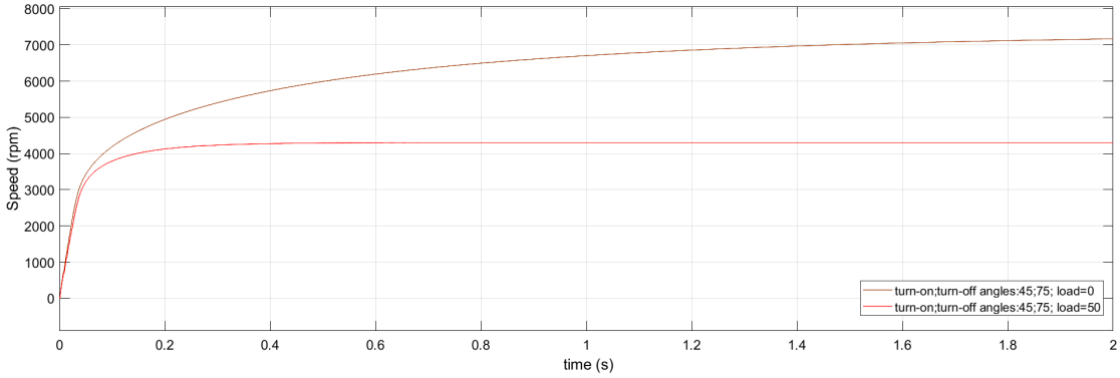

Figure 10. *Speed characteristics for operating mode with load and no-load operating mode at 45° and 75°*

From the no-load simulations where only the control angles are changed, one can derive the following conclusions:

- the steady-state flux is the greatest at the largest turn-on and turn-off (50°, 80°) angles and lowest at the smallest angles (40°, 70°);
- the current in the steady state is the smallest at the largest turn-on and turn-off (50°, 80°) angles and the highest at the smallest turn-on and turn-off angles (40°, 70°);
- the torque in the steady state is the largest at the smallest angles (40°, 70°), and at the largest angles (50°, 80°) we have a large decrease, i.e., the torque is the smallest. Also, there is a decrease in torque ripple when the turn-on and turn-off angles are 50°, 80, respectively, at the steady-state operation of the motor.
- The speed has the highest value at the smallest angles (40°, 70°) and the lowest at the largest angles (50°, 80°).

The largest speed and the torque of the motor are obtained for control angles 40 and 70. Up to the base speed of 3000 rpm, the motor torque is proportional to the current and constant for all presented control angles. Above the base speed, the torque decreases inversely with the speed. From stand still up to about 3000 rpm, the motor's emf is low and the current can be regulated to the reference value. In this operation mode, the average value of the developed torque is approximately proportional to the current reference. In

addition to the torque ripple due to phase transitions, we also note the torque ripple created by the switching of the hysteresis regulator. This operation mode is also called constant torque operation [5]. For speeds above 3000 rpm, the motor's emf is high and the phase currents cannot attain the reference value imposed by the current regulators. The converter operation changes naturally to voltage-fed mode in which there is no modulation of the power switches. They remain closed during their active periods and the constant DC supply voltage is continuously applied to the phase windings. This results in linear varying flux waveforms as shown on the scope. In the voltage-fed mode, the SRM develops its 'natural' characteristic in which the average value of the developed torque is inversely proportional to the motor speed. Since the hysteresis regulator is inactive in this case, only torque ripple due to phase transitions is present in the torque waveforms [5]. Above 3000 rpm, the control angles 40° and 70° allow the highest torque to be obtained, from all simulation models, and therefore the highest operational speed is obtained. Furthermore, in the SRM the speed is inversely proportional to the flux value related to the voltage supply; the smaller the flux, the bigger the motor speed is. This is the case when control angles are 40° and 70°. More details regarding the theoretical background of the relation between flux, speed and voltage in SRMs can be found in [1]. By an adequate selection of the control angles, various motor operating characteristics can be obtained that allow motor operation with various speeds. The control angles also have impact on the motor acceleration time. Yet, the torque ripple and the smooth operation of the motor are highly affected by the proper calculation of turn-off and turn-on angles. From the presented results it is evident that in case of turn-on and turn-of angles of 40° and 70° the torque ripple is high, contrary to the case with 50° and 80° control angles where the motor operation is smooth and torque ripple is low. In this paper, the control angles were arbitrarily chosen in the vicinity of the control angles of the base motor. Further authors' research should include analytical calculation of turn-off and turn-on angles and their impact on motor operating characteristics. For the turn-on turn-off angles of 45° and 75°, the load of 50 Nm is coupled to the motor shaft. From the results presented in Figure 10 and Table 1 and their comparison with the adequate results from Figure 8, it is evident that the motor acceleration time is longer due to the applied load, and the obtained speed is lower. Above the base speed, the motor current is slightly increased due to the applied load and motor operation on its 'natural' characteristic.

4. **Conclusion**

The main goal of this paper was to understand the operation of SRM and through simulations to present the impact of different turn-on and turn-off angles as well as the impact of the load on the transient characteristics of the motor. It can be concluded that by adding a load for the same turn-on and turn-off angles, a slight increase in flux, current and torque in the steady state operating mode can be observed, while the speed is reduced and the acceleration time is prolonged. Various turn-on and turn-off angles have significant impact on the motor speed and torque and their precise determination is highly important for the proper operation of the motor. Moreover, the torque ripple and motor smooth operation are highly affected by the proper determination of turn-off and turn-on angles. Therefore, authors' further research will be focused on the analytical calculation

of the optimum turn-off and turn-on angles for the optimal operation of the motor. The advantages of SRM are that this motor has a simple construction, high efficiency and reliability compared to conventional AC or DC motors and a high starting torque. The disadvantages of SRM are that the current versus the torque is very nonlinear, the phase shift must be precise to minimize the torque ripple and the phase current must be controlled to minimize the torque ripple.

References

[1] *Hughes, A. and Drury, B. (2013).* Electric Motors and Drives – Fundamentals, Types and Applications: Elsevier Ltd., book

[2] https://nit-edu.org/wp-content/uploads/2021/09/ch-39-Special-motors.pdf

[3] http://kaliasgoldmedal.yolasite.com/resources/SEM/SRM.pdf

[4] S. Abbasian (2013). Simulation and testing of a Switched Reluctance Motor by Matlab/Simulink and dSapce, Master Thesis, Faculty of Power Electrical Motors, Chalmers University, Goteborg, Sweden, available at: https://publications.lib.chalmers.se/records/fulltext/185186/185186.pdf

[5] Math Works (2022), https://www.mathworks.com/help/physmod/sps/ug/switched-reluctance-motor.html;jsessionid=53923789c96ee063f6946a8cd8b8

[6] H.E. Ahter, V.K. Sharma, A. Chandra, K.A. Hadad (2004). Determination of the optimum switching angles from speed control of switched reluctance motor driven system, Indian Journal of Engineering and Material Science, Vol. 11, pp. 151-168.

Sara Aneva
University of Goce Delchev Shtip,
Faculty of Electrical Engineering, Krste Misirkov 10-A
2000 Stip, Republic of North Macedonia
E-mail address: sara.20551@student.ugd.edu.mk

Vasilija Sarac
University of Goce Delchev - Shtip,
Faculty of Electrical Engineering, Krste Misirkov 10-A
2000 Stip, Republic of North Macedonia
E-mail address: vasilija.sarac@ugd.edu.mk